

***Ab initio* treatment of silicon defect clusters. The unrelaxed, neutral monovacancy**

J. C. Malvido and J. L. Whitten

*Department of Chemistry, State University of New York at Stony Brook,  
Stony Brook, New York 11794*

(Received 12 April 1982)

An embedding cluster theory is used to treat the neutral-vacancy defect in silicon by *ab initio* methods. Low-lying multiplets associated with the defect electrons are calculated by using accurate configuration-interaction expansions of the many-electron wave functions that include coupling to virtual (unoccupied) and bulk valence orbitals. It is found that for the nuclei in their unrelaxed positions, correlation effects are necessary to give the correct ordering among the fully covalent states:  ${}^1E(0.0 \text{ eV}) < {}^3T_1(0.1 \text{ eV}) < {}^5A_2(0.7 \text{ eV})$ . The partially ionic states  ${}^1T_2(3.6 \text{ eV}) < {}^1A_1(5.0 \text{ eV})$  are, in contrast, not sensitive to correlation corrections relative to the lower states.

**I. INTRODUCTION**

The single, isolated vacancy in an ideal silicon crystal has been treated by various formalisms for calculating the electronic properties of defects with strongly localized potentials. Within the last three years a number of sophisticated calculations based on the Green's-function method<sup>1,2</sup> have given a tangible picture of the defect orbitals.<sup>3-5</sup> The strength of the Green's-function method lies in its ability to reference the defect energy levels to the underlying electronic band structure of the solid. It is, therefore, essentially an effective one-electron theory subject to the same approximations used in constructing an effective one-electron Hamiltonian for the band.

Baraff, Schlüter, and collaborators have provided what is perhaps the most extensive analysis of the silicon vacancy, both as to the stability of the different charge states,<sup>6</sup> and more recently as to which competing effect dominates the ground state: electronic correlation or Jahn-Teller distortion.<sup>7</sup> They have resolved the multiplet splittings of given defect orbital configurations in terms of a few energy parameters that involve an exchange-correlation potential and conclude that the splitting is not negligible but is dominated by the Jahn-Teller effect. There is, however, no explicit inclusion of many-body effects via excitations to unoccupied spin orbitals, i.e., configuration interaction.

In early work Coulson and Kearsley introduced the concept of a "defect molecule"<sup>8</sup> to describe the electronic structure of the neutral vacancy in dia-

mond to which they attributed the observed absorption line below the main absorption edge in irradiated diamond. The model relates the electronic properties of the vacancy to the interaction of four unsaturated hybrid orbitals that intrude into the vacancy in what amounts to four electrons embedded in the fixed field of the crystal. An extension of this model to silicon by Surratt and Goddard<sup>9</sup> employs *ab initio* methods in evaluating the low-lying energy spectrum of the vacancy represented by a cluster of four silicon and twelve hydrogen atoms. The calculation unequivocally shows that correlation is an important factor in determining the correct multiplet ordering.

It has also been suggested in other one-electron studies that defect orbitals delocalize beyond the extent allowed by a small cluster model and that this delocalization leads to a reduction in the magnitude of the multiplet splitting<sup>6,7,10</sup>; furthermore, it is argued in the latter studies that correlations are overestimated in the *ab initio* cluster calculations.

The purpose of this paper is to examine quantitatively the problem of correlation in the unrelaxed, neutral vacancy with the use of an embedded cluster model that permits delocalization over the twelve nearest-neighbor atoms of the four atom plus vacancy complex. Emphasis is placed on two questions: how the multiplet structure depends on the level of sophistication of the many-electron treatment and how strongly bulk orbitals are polarized by the particular multiplet states of the vacancy electrons. The analysis in this work is essentially an adaptation of the localization concepts and

methods developed by Whitten and Pakkanen in discussing the chemisorption of gas molecules on a metal surface.<sup>11</sup> A new method is proposed for treating the boundary of the cluster that employs silicon atoms as saturators as opposed to the more customary practice of using hydrogen atoms.<sup>9,12</sup>

The paper is organized as follows: Section II reviews the theory of Ref. 11. Section III reports calculations on the silicon atom to establish limits on the accuracy of the treatment. Section IV gives an account of the cluster boundary model. Section V is devoted to an analysis of the unrelaxed, neutral silicon vacancy at both the self-consistent-field (SCF) and configuration-interaction (CI) levels. Finally, Sec. VI compares the present results with other theoretical studies and reports general conclusions.

## II. THEORY AND COMPUTATIONAL METHODS

The basic assumption is that the main chemical and physical changes associated with the defect involve the nearest-neighbor silicon atoms and that the influence of the more distant neighbors is perturbative. The defect is then simulated by a finite cluster of atoms where the defect site is surrounded by all the neighboring atoms of the host lattice, while the second or more distant neighbors are modeled to reflect the coupling of the cluster to the rest of the crystal. The present formulation involves conventional *ab initio* theory in developing a many-body approach for the electronic description of the defect, but at the same time introduces approximations that render a large cluster calculation tractable. Advantageous use is made of the localized form of the defect orbitals in constructing CI wave functions.

### A. Core-projected self-consistent-field theory

Hartree-Fock theory<sup>13,14</sup> is a convenient starting point for the analysis. Assuming that the  $1s$ ,  $2s$ , and  $2p$  core electrons are inert and representable by the atomic cores  $\{Q_m\}$ , the problem is then reduced to a study of the valence interactions in the presence of the Coulomb and exchange field of the frozen core, provided orthogonality to the core is maintained.

The core and valence one-electron density matrices can be expressed as sums over *occupied* spin orbitals

$$\gamma_c(1,2) = \sum_m Q_m(1)Q_m(2), \quad (1a)$$

$$\rho_c(1) = \gamma_c(1,1), \quad (1b)$$

$$\gamma_v(1,2) = \sum_i \psi_i(1)\psi_i(2), \quad (1c)$$

$$\rho_v(1) = \gamma_v(1,1). \quad (1d)$$

The Hamiltonian for the space of  $N_v$  valence electrons becomes

$$H_v = \sum_i^{N_v} h_i + \sum_{i<j}^{N_v} r_{ij}^{-1}, \quad (2)$$

and the total Hartree-Fock energy for the *valence* electrons is

$$E_v = \sum_i^{N_v} \langle \psi_i | h | \psi_i \rangle + \frac{1}{2} (\rho_v(1) | r_{12}^{-1} | \rho_v(2)) - \frac{1}{2} \langle \gamma_v(1,2) | r_{12}^{-1} | \gamma_v(1,2) \rangle, \quad (3)$$

where for  $P$  fixed nuclei

$$\begin{aligned} \langle \psi_i | h | \psi_i \rangle = & \left\langle \psi_i(1) \left| -\frac{1}{2} \nabla_1^2 - \sum_{k=1}^P \frac{Z_k}{r_{1k}} \right| \psi_i(1) \right\rangle \\ & + (\psi_i(1)\psi_i(1) | r_{12}^{-1} | \rho_c(2)) \\ & - \langle \psi_i(1)\psi_i(2) | r_{12}^{-1} | \gamma_c(1,2) \rangle. \end{aligned} \quad (4)$$

The valence orbitals are expanded in terms of valence basis functions  $X_p$ , which are orthogonal to core orbitals on the same center and Gramm-Schmidt orthogonalized to those on other centers to give

$$\psi_i = \sum_p C_{pi} X'_p, \quad (5a)$$

$$X'_p = X_p - \sum_m \langle Q_m | X_p \rangle Q_m. \quad (5b)$$

The coefficients  $C_{pi}$  in Eq. (5a) are obtained by solving the eigenvalue equation

$$\sum_q \langle X'_p | \tilde{F} | X'_q \rangle C_{qi} = \epsilon_i \sum_q S_{pq} C_{qi}, \quad (6a)$$

where

$$S_{pq} = \langle X'_p | X'_q \rangle, \quad (6b)$$

$$\begin{aligned} \langle X'_p | \tilde{F} | X'_q \rangle = & \langle X'_p | h | X'_q \rangle \\ & + (X'_p(1)X'_q(1) | r_{12}^{-1} | \rho_v(2)) \\ & - \langle X'_p(1)X'_q(2) | r_{12}^{-1} | \gamma_v(1,2) \rangle. \end{aligned} \quad (6c)$$

Equation (6a) follows by variation of Eq. (3) with respect to coefficient  $C_{pi}$  subject to the constraint  $\langle \psi_i | \psi_j \rangle = \delta_{ij}$ . Two key assumptions are now made that require inertness of the core orbitals:

$$\langle Q_m | Q_n \rangle = \delta_{mn} , \quad (7a)$$

$$\langle Q_m | \tilde{F} | Q_n \rangle = \epsilon_m \delta_{mn} . \quad (7b)$$

The core eigenvalue  $\epsilon_m$  need not be the atomic value, but may incorporate a shift due to the molecular environment. Introducing Eqs. (7a) and (7b) into (6a) leads to

$$\begin{aligned} \langle X'_p | \tilde{F} | X'_q \rangle &= \langle X_p | \tilde{F} | X_q \rangle \\ &\quad - \sum_m \epsilon_m \langle X_p | Q_m \rangle \langle Q_m | X_q \rangle , \end{aligned} \quad (8a)$$

$$S_{pq} = \langle X_p | X_q \rangle - \sum_m \langle X_p | Q_m \rangle \langle Q_m | X_p \rangle . \quad (8b)$$

In Eq. (8a) the second term on the right-hand side is effectively repulsive since  $\epsilon_m < 0$ . The first term, or Fock field, still depends on a valence Coulomb and exchange field constructed from the core-orthogonalized orbitals, but multicenter core-valence overlaps are small and thus these fields are constructed by projection onto the valence space. In Table I, typical numerical values of matrix elements of the type appearing in Eqs. (8a) and (8b) are tabulated.

The eigenvalue problem has the final (Phillips-Kleinman) form<sup>15</sup>

$$\sum_q \left\langle X_p \left| \left[ \tilde{F} - \epsilon_i - \sum_m (\epsilon_m - \epsilon_i) | Q_m \rangle \langle Q_m | \right] \right| X_q \right\rangle C_{qi} = 0 . \quad (9)$$

### B. Localization transformation and many-body treatment

The separation of molecular orbitals in a defect cluster calculation into bulk and defect orbitals is

conceptually useful and, as will be shown, qualitatively realistic. In a band-theoretic description, defect levels are found within a sizable fraction of the band-gap width away from either the conduction or valence edge. They become isolated from the bulk orbitals in the sense that different multiplet configurations of the defect state give rise to only small polarizations of the bulk orbitals.

There is then an effective decoupling of these levels from bulk orbitals so that correlation studies of defect-level electrons can be done independently of the rest of the crystal. It is thus possible as a first approximation to have excited states of the vacancy while the bulk remains in its ground-state configuration. This is the essence of the Coulson-Kearsley defect-molecule model. Nevertheless, configurational excitations from the bulk to empty defect levels and from the defect to the bulk can impart subtle relaxational many-body effects, and inclusion of such weak-coupling effects in this work is of interest.

A many-electron treatment of the defect levels can be developed by expanding the solution  $\Phi_\alpha$  [the Hamiltonian of Eq. (2)] as a linear combination of Slater determinants

$$\Phi_\alpha = \sum_\mu D_\mu^\alpha \Psi_\mu , \quad (10a)$$

where

$$\Psi_\mu = (N_v!)^{-1/2} \det | \psi_{\mu 1}(1) \psi_{\mu 2}(2) \cdots \psi_{\mu N_v}(N_v) | . \quad (10b)$$

The coefficients  $D_\mu^\alpha$  in Eq. (10a) are obtained by energy minimization of

$$\langle \Phi_\alpha | H_v | \Phi_\alpha \rangle = E_\alpha \langle \Phi_\alpha | \Phi_\alpha \rangle . \quad (11)$$

The molecular orbital set  $\{\psi_\mu\}$  in Eq. (10b) is derived from the SCF solution and includes both occupied and virtual orbitals. The size of this set may be such as to make a full CI expansion computationally prohibitive.

TABLE I. Typical matrix elements in  $\text{Si}_{17}$ . Energies are in atomic units (1 a.u. = 27.21 eV). Subscripts 1 and 2 refer to different nuclei, 4.44 a.u. internuclear distance. Summations are over all core orbitals on all nuclei of  $\text{Si}_{17}$ ; one-center contributions are zero due to orthogonality.

$ a\rangle,  b\rangle$	$\langle a   \tilde{F}   b \rangle$	$-\sum_m \epsilon_m \langle a   Q_m \rangle \langle Q_m   b \rangle$	$\langle a   b \rangle$	$\sum_m \langle a   Q_m \rangle \langle Q_m   b \rangle$
$3s_1, 3s_1$	-0.625	0.0251	1.00	0.0041
$3p_1, 3p_1$	-0.395	0.082	1.00	0.0126
$3s_1, 3s_2$	-0.219	$0.224 \times 10^{-3}$	0.235	$0.333 \times 10^{-4}$
$3s_1, 3p_2$	-0.162	$0.885 \times 10^{-3}$	0.227	$0.147 \times 10^{-3}$

Since it is the correlation among the defect-level electrons that is of interest, these levels can be singled out as the chief source of excitations. Different classes of excitations that have a bearing on the CI expansion, arranged in order of importance, are as follows:

(a) Spin and orbital-occupation changes among the defect levels (to describe multiplet energy splittings).

(b) Excitations from defect levels to virtual levels (to introduce spatial correlations and especially the proper ionic-covalent character in bonds).

(c) Excitations from deep valence levels to empty defect levels (to permit further relaxation of the defect and bulk).

To aid in the selection of orbitals for correlation purposes, a localization transformation is performed. Defect orbitals are arranged into a *reference* density matrix

$$R(1,2) = \sum_i \psi_i^d(1) \psi_i^d(2). \quad (12)$$

A new set of orbitals is then formed by a linear transformation of the occupied and virtual spaces separately:

$$\psi_i^\sigma = \sum_p \Lambda_{pi}^\sigma \psi_p^\sigma, \quad (13a)$$

$$\psi_i^v = \sum_p \Lambda_{pi}^v \psi_p^v. \quad (13b)$$

Coefficients  $\Lambda_{ij}^{\sigma,v}$  are obtained by maximizing the positive-definite exchange integral

$$\lambda_i^{\sigma,v} = \langle \psi_i^{\sigma,v}(1) \psi_i^{\sigma,v}(2) | r_{12}^{-1} | R(1,2) \rangle \geq 0. \quad (14)$$

The resulting matrix-eigenvalue problem yields a spectrum  $\lambda_1^{\sigma,v} \geq \lambda_2^{\sigma,v} \geq \dots \geq \lambda_p^{\sigma,v}$  that corresponds to the exchange between the orbitals  $\psi_i^{\sigma,v}$  and those of the reference density matrix.<sup>11</sup> The exchange between two-electron distributions is a measure of their interpenetration. By taking the relative magnitude of different eigenvalues as a measure of the coupling of  $\psi_i^{\sigma,v}$  to the defect orbital density Eq. (12), we can use the eigenvalues as a criterion to select orbitals to be included in the CI expansion. Occupied orbitals excluded from excitation become part of the CI core, and virtual orbitals with "small" exchange eigenvalues are discarded. The remaining orbitals are part of an "active" CI basis.

Since the transformation [Eqs. (13a) and (13b)] is unitary, the total energy and wave function of the SCF solution

$$\Psi_{\text{SCF}} = (N_v!)^{-1/2} \det | \psi_1(N_v) \cdots \psi_{N_v}(N_v) | \quad (15)$$

are invariant. Upon transformation

$$\begin{aligned} \Psi'_{\text{SCF}} = & (N_v!)^{-1/2} \det | \psi_1^\sigma(1) \cdots \psi_m^\sigma(m) \\ & \times \psi_{m+1}^\sigma(M+1) \cdots \psi_{N_v}^\sigma(N_v) | \end{aligned} \quad (16)$$

where  $\psi_1^\sigma, \dots, \psi_m^\sigma$  represent the active CI basis; and  $\psi_{m+1}^\sigma, \dots, \psi_{N_v}^\sigma$ , the occupied CI core orbitals.

This transformed wave function is used as a starting point for CI excitations between the active occupied and virtual set. Configurations  $\Psi_\mu$  are generated via single and double excitations from the active subspace of  $\Psi'_{\text{SCF}}$  and retained if they satisfy the interaction criterion

$$\frac{|\langle \Psi_\mu | H_v | \Psi'_{\text{SCF}} \rangle|^2}{E_\mu - E_{\text{SCF}}} > 10^{-5}. \quad (17)$$

The eigenstates are then obtained by diagonalization of the Hamiltonian. If any of the configurations  $\Psi_\mu$  have coefficients  $D_\mu^\alpha > 10^{-1}$ , these are then included as reference configurations from which additional excitations are carried out thereby enlarging the scope of the expansion. In this work the low-lying states are expanded with up to  $\sim 700$  configurations. The diagonalization is done recursively as described in Ref. 16.

### III. BASIS SET

#### A. Silicon atom and diatom

Expansion of atomic orbitals as a sum of weighted gaussians of different decay constants are widely used in molecular and band-type solid calculations. Dunning and Hay<sup>17</sup> review some of the technical aspects of Gaussian expansions appropriate to molecular calculations as well as include an extensive bibliography of various basis sets of near Hartree-Fock quality for the first three rows of the Periodic Table.

The atomic orbital expansions used in this work have the radial form

$$X(r) = \sum_i C_i (2\alpha_i/\pi)^{3/4} e^{-\alpha_i r^2}, \quad (18)$$

and the angular dependence is introduced via the Gaussian lobe method.<sup>18</sup> For the description of the silicon atom, we have used the basis set derived by

Roos and Siegbahn.<sup>19</sup> Their expansion uses ten  $s$ -type and six  $p$ -type Gaussians optimized for the  $^3P$  ground state with the shell structure  $1s^2 2s^2 2p^6 3s^2 3p^2$ .

A practical advantage is gained by fitting the valence orbitals with smaller expansions in which spatially contracted Gaussians are utilized to achieve orthogonality to the core, and the diffuse tail is reproduced accurately. Accurate expansions for the  $1s$ ,  $2s$ , and  $2p$  orbitals that are needed to compute the valence-core overlap matrix elements [see Eqs. (8a) and 8(b)] are retained. Valence orbitals  $3s$  and  $3p$  are fitted by a five- or four-term exponent, respectively, with a least-squares procedure. Small adjustments to the more contracted Gaussians in this fit are made in order to maintain strict orthogonality to the core ( $\sim 10^{-6}$ ). In Table II the different bases are compared as to eigenvalues and total energy. The core eigenvalues are well reproduced, but the fitting procedure has introduced an error of  $<0.01$  a.u. to the valence eigenvalues and  $0.05$  a.u. to the total energy.

To restore flexibility to the valence space, an auxiliary basis (double zeta) is introduced, consisting of a three-term  $s$ -type and two-term  $p$ -type orbital ( $3s', 3p'$ ) in which the most diffuse component of the fitted  $3s$  and  $3p$  is retained and orthogonalized to the core. A valence-only calculation is performed, including one where the exact core density is replaced by a simplified expansion of the form of Eq. (18). These results are in Table III.

The valence configuration  $3s^2 3p^2$  gives rise to three closely spaced multiplets  $^3P$ ,  $^1D$ , and  $^1S$ , with representative components of the minimal configurational representation as follows:

TABLE II. Atomic eigenvalues and total energy for silicon.

		Orbital Energies (a.u.)		
		Basis <sup>a</sup>	Basis <sup>b</sup>	Basis <sup>c</sup>
Core	$1s$	-68.811	-68.792	-68.798
	$2s$	-6.155	-6.136	-6.137
	$2p$	-4.255	-4.228	-4.225
Valence	$3s$	-0.539	-0.526	-0.515
	$3p$	-0.296	-0.284	-0.271
Total energy		-288.854	-288.773	-288.724

<sup>a</sup>Hartree-Fock quality (Ref. 20).

<sup>b</sup>Roos-Siegbahn (Ref. 19).

<sup>c</sup>Fitted valence and core from Roos-Siegbahn (Ref. 19).

$$^3P: \frac{1}{\sqrt{2}} ( |p_x \bar{p}_y \rangle + | \bar{p}_x p_y \rangle ), \quad (19a)$$

$$^1D: \frac{1}{\sqrt{2}} ( |p_x \bar{p}_y \rangle - | \bar{p}_x p_y \rangle ), \quad (19b)$$

$$^1S: \frac{1}{\sqrt{3}} ( |p_x \bar{p}_x \rangle + |p_y \bar{p}_y \rangle + |p_z \bar{p}_z \rangle ). \quad (19c)$$

The splittings at the Hartree-Fock level calculated from properties of the Slater determinants, assuming a common set of orbitals, are<sup>21</sup>

$$\Delta(^1D-^3P) = (p_x p_x || p_x p_x) - (p_x p_x || p_y p_y) \quad (20a)$$

$$= 2(p_x p_y || p_x p_y), \quad (20b)$$

$$\Delta(^1S-^3P) = 5(p_x p_y || p_x p_y), \quad (20c)$$

where the equivalent expression for  $\Delta(^1D-^3P)$  is a consequence of rotational symmetry; ( $||$ ) denotes the electron order 11,22. Experimental values<sup>22</sup> and calculated SCF values (in parentheses), expressed in a.u. are as follows:

$$\Delta(^1D-^3P) = 0.028(0.0410), \quad (21a)$$

$$\Delta(^1S-^3P) = 0.070(0.1025). \quad (21b)$$

CI calculations were carried out using the double-zeta valence basis and in a separate series by including single Gaussian  $d$  orbitals ( $\alpha=0.12$ ). The CI lowering favors the  $^1S$  description, which interacts strongly with configurations derived by double excitations from the  $3s$  to the empty  $3p$  level. Inclusion of the  $d$  orbitals, on the other hand, favors the  $^3P$  and  $^1D$ , with the  $^1D$  gaining only  $0.003$  a.u. over the  $^3P$ . This level of treatment has

TABLE III. Valence eigenvalues and energies.

	Orbital energies (a.u.)		
	Basis <sup>a</sup>	Basis <sup>b</sup>	Basis <sup>c</sup>
$3s$	-0.526	-0.526	-0.518
$3p$	-0.284	-0.279	-0.275
Valence energy	-3.665	-3.619	-3.620

<sup>a</sup>Roos-Siegbahn basis (Ref. 19).

<sup>b</sup>Double-zeta.

<sup>c</sup>Approximate core expansion.

therefore given the splitting

$$\Delta(^1D-^3P)=0.038, 0.041, \quad (22a)$$

$$\Delta(^1S-^3P)=0.081, 0.070, \quad (22b)$$

with and without  $d$ -orbital excitations, respectively.

Thus, use of additional diffuse  $s$  and  $p$ -like orbitals together with the  $d$  orbitals led to a considerable improvement in the  $\Delta(^1S-^3P)$  splitting, but did not affect the  $\Delta(^1D-^3P)$  splitting. This indicates that the  $^1S$  contains some Rydberg character.

#### B. Diatomic calculations—molecule optimized basis

Calculations on  $\text{Si}_2$  employing a double-zeta basis were analyzed in order to derive a more optimal minimal basis for use on cluster atoms outside the vacancy region. Atomic orbitals derived from an  $sp^3$  state of the Si atom were found to reproduce the double-zeta  $\text{Si}_2$  results as shown in Table IV.

#### IV. BOUNDARY MODEL—APPLICATIONS TO THE $\text{Si}_{17}$ CLUSTER

A number of silicon-cluster calculations have been reported in the literature.<sup>9,13,23</sup> Boundary conditions have been simulated by surrounding the cluster with hydrogen atoms so as to saturate the bonding. This approach is appealing due to its simplicity and the fact that the electronegativities for hydrogen and  $sp^3$  silicon are similar.

An alternative formulation of boundary conditions is considered here that is generalizable to other covalent monatomic or compound clusters. The "boundary model" assumes an  $sp^3$ -hybridized valence shell in which the four electrons are distributed equally among the  $s$ ,  $p_x$ ,  $p_y$ , and  $p_z$  valence

TABLE IV.  $\text{Si}_2$ -basis comparison.

	Energies (a.u.)	
	Optimized minimal	Double-zeta
$\sigma_1$	-0.662	-0.662
$\sigma_2$	-0.455	-0.457
$\pi_1, \pi_2$	-0.253	-0.253
Total energy	-6.423	-6.424

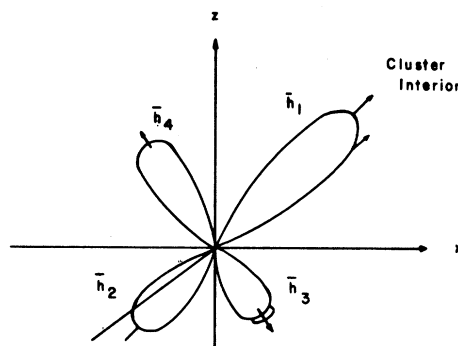
orbitals. One convenient representation of the assumed  $sp^3$ -hybrid structure is depicted in Fig. 1. The boundary model is then constructed as follows:

(a) The hybrid  $\bar{h}_1$  is directed along a tetrahedral bond axis into the interior of the cluster (Fig. 1). The  $s$ - $p$  ratio is kept fixed, but the hybrid combination is otherwise free to mix variationally with interior orbitals.

(b) The back bond  $\bar{h}_2$  is maintained invariant and provides a Coulomb and exchange field equivalent to that of a single electron with an averaged spin. Interior orbitals are orthogonalized to  $\bar{h}_2$ , but otherwise no further mixing occurs.

(c) Hybrids  $\bar{h}_3$  and  $\bar{h}_4$  are replaced by an effective potential which conserves charge (2 electrons) and maintains the correct polarity of the bond involving  $\bar{h}_1$  and the interior atoms.

The potential on the boundary atoms is chosen to make the Si—Si bond nonpolar at the bulk lattice distance. Table V gives eigenvalues and Mulliken populations on the  $3s$  and  $3p$  basis orbitals for two sets of calculations. In (a) only  $\bar{h}_{1a}$  and  $\bar{h}_{1b}$  (see Fig. 2) are allowed to mix; other hybrids are constrained to be singly occupied (spin averaged). The  $\sigma_1$  and  $\sigma_1^*$  bonds correspond to the linear combinations



$$\left. \begin{aligned} \bar{h}_1 &= \frac{1}{2}s + \frac{\sqrt{3}}{2}p_{\parallel} \\ \bar{h}_2 &= \frac{\sqrt{3}}{2}s - \frac{1}{2}p_{\parallel} \end{aligned} \right\} p_{\parallel} = \frac{1}{\sqrt{3}}(p_x + p_y + p_z)$$

$$\bar{h}_3 = \frac{1}{\sqrt{2}}(p_x - p_y)$$

$$\bar{h}_4 = \frac{1}{\sqrt{6}}(p_x + p_y - 2p_z)$$

FIG. 1.  $sp^3$  hybrid model for the boundary.  $\bar{h}_1$  mixes with interior orbitals,  $\bar{h}_2$  invariant, and  $\bar{h}_3$  and  $\bar{h}_4$  replaced by an effective potential.

TABLE V. Hybrid bond model orbital eigenvalues and Mulliken populations.

	Energies (a.u.)	
	Constrained occupancy <sup>a</sup>	Effective potential <sup>b</sup>
$\sigma_1$	-0.498	-0.470
$\sigma_1^*$	0.222	0.235
Populations		
(3s)	0.945	0.945
(3p)	1.055	1.055

<sup>a</sup>Mixing of  $\bar{h}_{1a}$  and  $\bar{h}_{1b}$  only; other hybrids singly occupied (Fig. 2).

<sup>b</sup>Mixing of  $h_{1a}$  and  $h_{1b}$  only; hybrids  $\bar{h}_{3b}$  and  $\bar{h}_{4b}$  replaced by an effective density.

$$\sigma_1 = (\bar{h}_{1a} + \bar{h}_{1b})(2 + 2S_{ab})^{-1/2}, \quad (23a)$$

$$\sigma_1^* = (\bar{h}_{1a} - \bar{h}_{1b})(2 - 2S_{ab})^{-1/2}. \quad (23b)$$

In (b) the hybrids  $\bar{h}_{3b}$  and  $\bar{h}_{4b}$  were replaced by the density

$$\rho = 0.01983 \exp(-0.145r^2), \quad (24)$$

which integrates to two electrons, and as seen from the results this gives an accurate reproduction of the bonding and antibonding orbital eigenvalue splitting as well as preserves the proper 3s-3p population balance.

The boundary model was also tested in a 17-Si-atom minimal basis cluster calculation. The geometry is tetrahedral and the distances are those of bulk of silicon; the cluster is depicted in Fig. 3. Each of five central atoms has 3s, 3p<sub>x</sub>, 3p<sub>y</sub>, and 3p<sub>z</sub> valence orbitals, the twelve surrounding silicon atoms are modeled as described above—a 3s and 3p<sub>||</sub> (along the bond axis) orbital, plus an effective density.

The eigenvalue spectrum is shown in Fig. 4 along with the Mulliken populations of the central (c), nearest-neighbor (NN), and boundary (b)

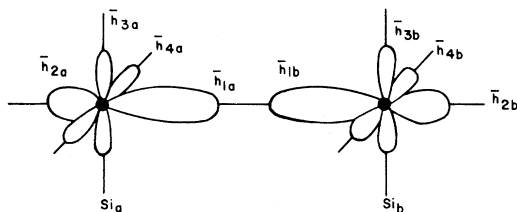


FIG. 2. Si<sub>2</sub> model to check bond polarity.  $\bar{h}_{3b}$  and  $\bar{h}_{4b}$  are replaced by an effective potential so that charge is equally shared by  $\bar{h}_{1a}$  and  $\bar{h}_{1b}$ .

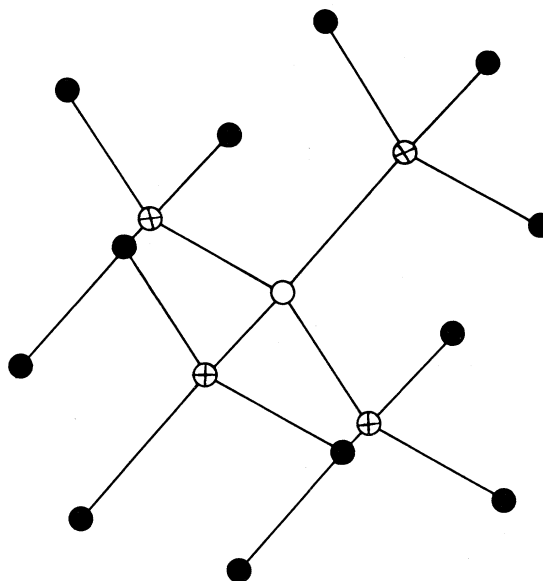


FIG. 3. Cluster model.  $\circ$ , center atom (missing in vacancy calculation);  $\otimes$ , neighboring atom;  $\bullet$ , boundary atom.

atoms. It is seen that there is a slight departure in the interior atoms from the ideal  $sp^3$  distribution, and a net loss of  $\sim 0.05$  electrons per boundary atom that probably enhances the  $s$  population in the interior. In part, these shifts are due to the cluster itself since the interior atoms are in a deeper potential well than the boundary atoms. The charge shifts in any case are small and are within the uncertainty of the Mulliken partitioning.

Kane and Kane have variationally determined Wannier representations for the silicon valence bands using simple parametrized potentials.<sup>23</sup> Summations over a specified number of neighbor shells and inequivalent bonds are carried out to check convergence of Wannier energy sums to the Bloch eigenvalues. In the Bloch representation the  $\Gamma_1$  and  $\Gamma_{25'}$  symmetry points correspond to the lowest and the highest energies, respectively, in the valence band. In our calculation these would correspond to the  $1a_1$  and  $3t_2$  energy levels which are primarily  $s$  type for  $1a_1$  and primarily  $p$  type for  $3t_2$  just as in the band case.<sup>24</sup> Assuming this correspondence, we find their value at these two symmetry points to be  $-0.760$  and  $-0.313$  a.u., respectively, when they sum over three neighbor shells and eight inequivalent bonds. This summation coincides with the size of the Si<sub>17</sub> cluster, and as we see from Fig. 4 the energies match very

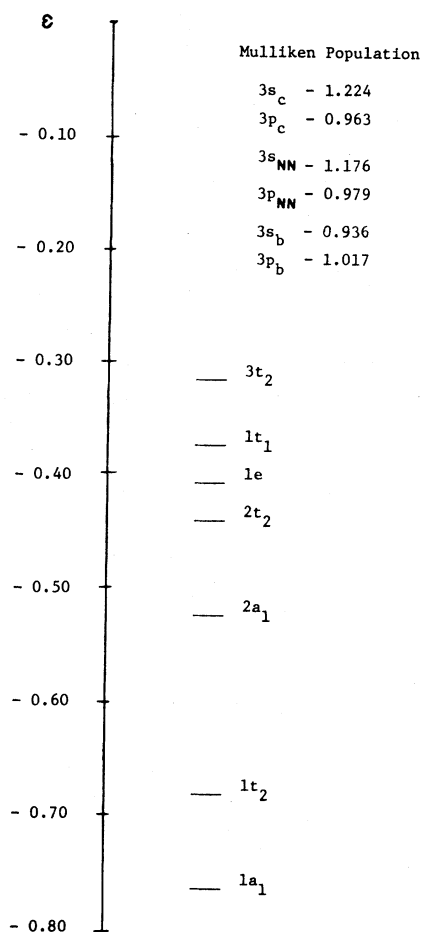


FIG. 4.  $\text{Si}_{17}$ : eigenvalue spectrum of occupied orbitals (a.u.) and Mulliken populations of central (c), nearest-neighbor (NN) and boundary atoms (b).

closely ( $-0.759$  and  $-0.313$  a.u. for  $1a_1$  and  $3t_2$ , respectively).

The valence-band width as determined by the difference between the same eigenvalues is 0.45 a.u., or 12.2 eV. This compares very well with the value reported by pseudopotential band calculations.<sup>25,26</sup> Optical transitions  $\Gamma_{25'}-\Gamma_{15}$  and  $L_3-L_1$  are both of the order of 3.5 eV.<sup>25</sup> We can obtain an estimate of the energy of the  $3t_2-4t_2$  excitation by assuming that the calculated levels are rigid to an electronic transition. If this is the case, then the energy of transition is given by

$$\Delta E = \epsilon_{n+1} - \epsilon_n - J_{n,n+1}, \quad (25a)$$

where

$$J_{n,n+1} = (\psi_n(1)\psi_n(1) | r_{12}^{-1} | \psi_{n+1}(2) \times \psi_{n+1}(2)). \quad (25b)$$

Equation (25a) is equivalent to that of an excited electron interacting with its hole. In our calculations  $J_{n,n+1} = 0.175$  a.u. so that  $\Delta E = 0.282$  a.u., or 7.67 eV, i.e., more than twice the experimental value. Examination of the  $4t_2$  orbital shows that over 30% of its charge density comes from the boundary as opposed to 8% for the  $3t_2$  orbital. The  $4t_2$  is thus spatially extended, and its optimization would require a larger cluster and a more extended basis description.

Kenton and Ribarsky<sup>27</sup> use the hydrogen saturator model in calculating energy levels for a  $\text{Si}_3\text{H}_{12}$  cluster. Their results give the same ordering of levels and energy width between the  $1a_1$  and  $3t_2$ , which suggests that this width is largely determined by the nearest-neighbor interaction. There are, however, discrepancies of as much as 0.05 a.u. in the magnitude of the eigenvalues, with their levels tending to be lower. In particular, their  $3t_2$  level merges with the  $1t_1$  and  $1e$  level when they use hydrogen at the Si-Si distance, a feature not shown by our calculations. Since no  $p$  orbitals are present in the hydrogen saturator model, there is no direct bond. This may affect the energy, even though it has little effect on the electron density in the interior of the cluster.

## V. UNRELAXED VACANCY

### A. SCF calculations

The geometry of the unrelaxed vacancy is identical to that of the  $\text{Si}_{17}$  cluster, but the central atom is now missing. The double-zeta basis described in Sec. IV is used to span the four atoms neighboring the vacancy. There are, in addition, four one-term Gaussians of  $s$  and  $p$  symmetry at the vacancy site with exponent  $\alpha = 0.1$ . The surrounding twelve atoms are described as in the  $\text{Si}_{17}$  calculation. The valence potential used for these boundary atoms has also been shown to give the proper mixing of the double-zeta basis for  $\text{Si}_2$ .

Removal of the center atom leaves four partially occupied orbitals (dangling bonds) labeled  $h_a, \dots, h_d$  in Fig. 5. Transformed orbitals belonging to the  $A_1$  and  $T_2$  irreducible representations of the tetrahedral group are as follows:

$$a_1 = (h_a + h_b + h_c + h_d)(4 + 12S)^{-1/2}, \quad (26a)$$

$$t_{2x} = (h_a - h_b - h_c + h_d)(4 - 4S)^{-1/2}, \quad (26b)$$

$$t_{2y} = (h_a - h_b + h_c - h_d)(4 - 4S)^{-1/2}, \quad (26c)$$

$$t_{2z} = (h_a + h_b - h_c - h_d)(4 - 4S)^{-1/2}, \quad (26d)$$

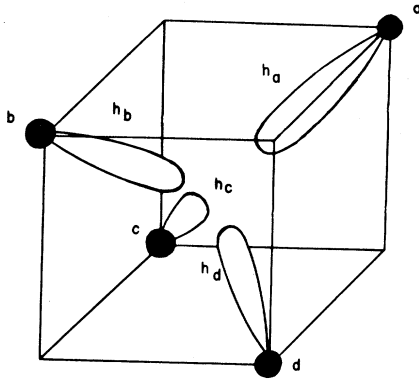


FIG. 5. Dangling bonds around vacancy site. The  $s$ - $p$  ratio is calculated self-consistently.

where hybrid orbitals, which can differ in  $A_1$  and  $T_2$ , are to be determined self-consistently.

The  $(a_1^2 t_2^2)$  configuration gives rise to the multiplet sequence  ${}^1E$ ,  ${}^3T_1$ ,  ${}^1T_2$ , and  ${}^1A_1$ . The  $S_z=0$  components have the form

$${}^1E: \frac{1}{\sqrt{2}} (|a_1 \bar{a}_1 t_x \bar{t}_x\rangle - |a_1 \bar{a}_1 t_y \bar{t}_y\rangle), \quad (27a)$$

$${}^3T_1: \frac{1}{\sqrt{2}} (|a_1 \bar{a}_1 t_x \bar{t}_y\rangle + |a_1 \bar{a}_1 \bar{t}_x t_y\rangle), \quad (27b)$$

$${}^1T_2: \frac{1}{\sqrt{2}} (|a_1 \bar{a}_1 t_x \bar{t}_y\rangle - |a_1 \bar{a}_1 \bar{t}_x t_y\rangle), \quad (27c)$$

$${}^1A_1: \frac{1}{\sqrt{3}} (|a_1 \bar{a}_1 t_x \bar{t}_x\rangle + |a_1 \bar{a}_1 t_y \bar{t}_y\rangle + |a_1 \bar{a}_1 t_z \bar{t}_z\rangle). \quad (27d)$$

The  ${}^5A_2$  state is derived from a  $(2a_1 3t_2^3)$  configuration:

$${}^5A_2: \frac{1}{\sqrt{6}} (|a_1 t_x \bar{t}_y \bar{t}_z\rangle + |\bar{a}_1 \bar{t}_x t_y t_z\rangle + |a_1 \bar{t}_x \bar{t}_y t_z\rangle + |\bar{a}_1 t_x t_y \bar{t}_z\rangle + |a_1 \bar{t}_x t_y \bar{t}_z\rangle + |\bar{a}_1 t_x \bar{t}_y t_z\rangle). \quad (27e)$$

In addition, an averaged configuration occupancy (the same as in Ref. 5) is defined by assigning one third of an electron to each of the six  $3t_2$  spin orbitals. The resulting symmetric field provides a convenient reference for the analysis of the different CI expansions. Converged SCF solutions were obtained for the  ${}^3T_1$ ,  ${}^1T_2$ , and  ${}^5A_2$  states as well as for the averaged configuration occupancy. Figure 6 shows the calculated energy levels for each case and also levels of  $\text{Si}_{17}$  for comparison.

The most evident shifts are associated with the  $1a_1$ ,  $2a_1$ , and  $3t_2$  orbitals, which in  $\text{Si}_{17}$  contain an appreciable population on the central atom. The  $1a_1$  orbital spreads outward toward the boundary, while the  $2a_1$  and  $3t_2$  orbitals have densities concentrated on nearest neighbors of the vacancy. We refer to the latter orbitals,  $2a_1$  and  $3t_2$ , as the defect orbitals. The other orbitals experience only minor shifts ranging from 0.15 eV for the  $1t_1$ ,  $1e$ , and  $2t_2$  orbitals to 0.70 eV for the  $1t_2$  orbital, or  $\leq 5\%$  of the bandwidth (these orbitals together with  $1a_1$  will be referred to as bulk orbitals). Though significant charge rearrangement takes place within each orbital, the total valence population per atom remains unchanged from the bulk result of four valence electrons per atom.

The  ${}^3T_1$  and  ${}^1T_2$  calculations converged rapidly when the converged field from the averaged configuration was used as a starting iterative field. There were no discernible shifts in the eigenvalue spectrum of the bulk and  $2a_1$  orbitals for the  ${}^3T_1$  optimization. Uniform downward eigenvalue shifts of the order of 0.08 eV occurred in the same orbitals in the case of the  ${}^1T_2$  optimization, which is evidence of polarization effects due to specific open-shell structure in the vacancy region. The defect  $3t_2$  level of the averaged configuration occurs high in the eigenvalue spectrum due to the physically incorrect averaged field.

The energy splitting of the optimized  ${}^3T_1$  and  ${}^1T_2$  states is calculated to be 2.79 eV at the SCF level. With the use of the defect orbitals from the averaged configuration, the splitting given by  $2\langle t_{2x}^{(1)} t_{2y}^{(1)} || t_{2x}^{(2)} t_{2y}^{(2)} \rangle$  is essentially the same numerically, 2.82 eV. It is noted, however, that the difference in  $3t_2$  eigenvalues  $\epsilon({}^1T_2) - \epsilon({}^3T_1)$  is 2.61 eV; if all orbitals were unchanged from those of the averaged configuration, the energy splitting and the eigenvalue difference would be the same. Since the discrepancy is very small, these results suggest that a CI expansion for the total energy can be carried out using the averaged configuration as a reference basis.

Optimized orbitals for the  ${}^5A_2$  state lead to upward shifts of 0.13 and 0.05 eV for the  $1a_1$  and  $1t_2$ , respectively; other bulk orbitals were also shifted upward on the average by 0.02 eV with respect to those of the averaged configuration. Both defect orbitals are lowered in energy due to the redistribution of electrons. The total energy difference between the optimized  ${}^5A_2$  and the energy of the same state using the orbitals from the averaged configuration is 0.33 eV. The same comparison for the  ${}^3T_1$  and  ${}^1T_2$  states gives a differ-

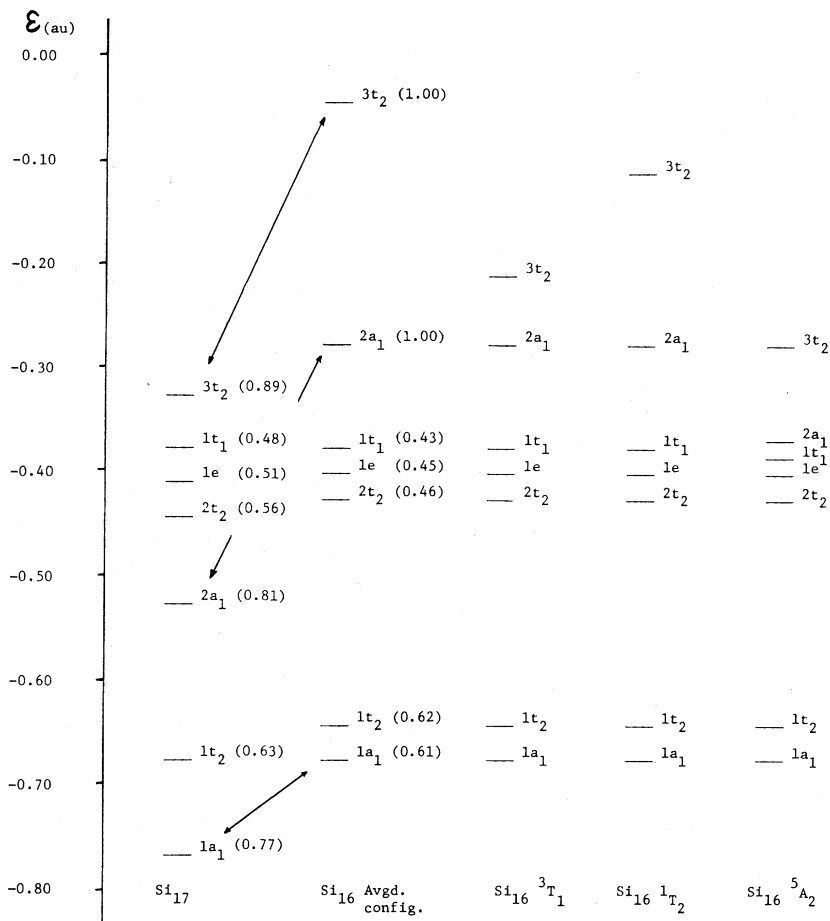


FIG. 6. Eigenvalue spectra of  $\text{Si}_{16}$  vacancy states and  $\text{Si}_{17}$ . Values in parentheses are total Mulliken populations of basis functions in the vacancy (or the central atom in  $\text{Si}_{17}$ ) and on the four neighboring atoms.

ence of only 0.03 eV, so the possibility exists that a CI expansion for the  ${}^5A_2$  in terms of the basis of averaged configuration orbitals will converge more slowly. The present SCF calculations show some bulk orbital polarization especially for the  ${}^3T_1$  and  ${}^5A_2$  states; these small relaxations are included in the CI treatments by allowing excitations from the bulk orbitals.

### B. Localization transformation

The purpose of the localization transformation is to reorder orbitals defining the occupied and virtual spaces, separately, according to the magnitude of the exchange with the defect reference density (see Sec. III B). Transformed orbitals with a large exchange will penetrate significantly into the vacancy region, while those with small exchange will lie principally outside the vacancy region. This distinction is operationally useful if one is interested

in refining mainly the description of the vacancy region.

The vacancy reference density is defined with the use of the defect orbitals  $2a_1$  and  $3t_2$  as components. The transformation is carried out separately for the occupied and virtual spaces. In the occupied-space transformation the partially filled  $3t_2$  orbitals are excluded. The resulting exchange energy spectrum is given in Fig. 7 along with a symmetry classification of the orbitals and a tabulation of the vacancy region populations. The localized orbitals fall into three groups. The largest exchange eigenvalues are associated with the  $3t_2$  ( $\lambda_{1t_2}$ ) and  $2a_1$  ( $\lambda_{1a_1}$ , which actually contains a 1%  $1a_1$  admixture) orbitals. The second group has an eigenvalue range of 0.025–0.005 a.u.; it includes four occupied and twelve virtual orbitals involving the four atoms bordering the vacancy. Orbitals in the third group all have eigenvalues less than 0.005 a.u. Active orbitals for the CI ex-

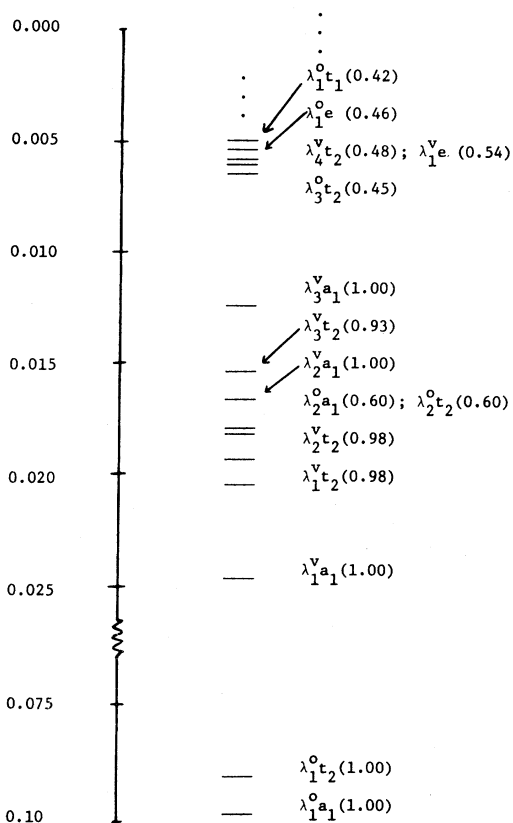


FIG. 7. Orbital exchange eigenvalue spectrum and total Mulliken population on the four atoms neighboring the vacancy and on basis functions in the vacancy.

pansion are taken to include all members of the first two groups plus occupied orbitals in the third group with symmetry  $e$  and  $t_1$  included so as to allow excitations from these symmetries.

### C. CI results

Multiplet splittings (in a.u.) for the states [Eqs. (27)] calculated using the averaged configuration orbitals and a minimal determinantal representation are as follows:

$$E(^1E) - E(^3T_1) = (t_x t_x | | t_x t_x) - (t_x t_x | | t_y t_y) \\ = 0.0010 ,$$

$$E(^1T_2) - E(^3T_1) = 2(t_x t_y | | t_x t_y) \\ = 0.1026 ,$$

$$E(^1A_1) - E(^1E) = 3(t_x t_y | | t_x t_y) \\ = 0.1539 ,$$

$$E(^5A_2) - E(^3T_1) = -0.0400 .$$

Thus, the  $^5A_2$  state is lowest in energy followed by  $^3T_1$ ,  $^1E$ ,  $^1T_2$ , and  $^1A_1$  states. If excitations among only the defect levels are allowed, the  $^1E$  and  $^3T_1$  are inverted and both drop below the  $^5A_2$  state. Two additional stages of configuration interaction are carried out: first, inclusion of excitations to all virtual levels from the defect orbitals and second, inclusion of excitations from bulk orbitals to unoccupied defect orbitals. In the latter calculations, excited configurations are generated from the determinants that contribute significantly to the defect-orbital-only CI expansion. For example, in the determination of the  $^3T_1$  and  $^1T_2$  states a total of four parent configurations was used to generate a total of 766 configurations.

The CI results are tabulated in Table VI. The reported values are relative to the SCF energy of the  $^1E$  state. The evolution of the energy splitting of the various states for the different stages of CI treatment is depicted in Fig. 8. Energy lowerings of the  $^1E$  and  $^3T_1$  are greater than the lowering of the  $^1T_2$  and  $^1A_1$  states by almost 0.9 eV. The  $^5A_2$  state has been treated differently. Since the averaged configuration orbitals do not provide a good starting point for representation of the  $^5A_2$  state in Fig. 8 the  $^5A_2$  state is shifted downward by 0.33 eV, which is the error at the SCF stage on use of the average configuration orbitals. The effect of this is to overestimate slightly the stability of the  $^5A_2$  state.

### D. Analysis of the $^3T_1$ - $^1T_2$ energy splitting

In this section we examine the electronic distribution of the  $^3T_1$  and  $^1T_2$  states and relate the electronic structure to the magnitude of the splitting of these states. Although the main components of the triplet and singlet states differ only in sign between the spin-complement determinant pairs, the states exhibit markedly different characteristics of electronic correlation. The  $^3T_1$  state derives 80% of the calculated correlation energy via excitations among defect orbitals. In contrast the  $^1T_2$  state derived 60% of its correlation from defect orbital excitations and about 25% from interactions with virtual orbitals.

An essential difference between the  $^3T_1$  and  $^1T_2$  states can be demonstrated by expansion of the two determinant pairs, Eqs. (27b) and (27c), and expression of the open shell contributions in terms of hybrid orbitals  $h_a$ ,  $b_b$ ,  $h_c$ , and  $h_d$ , viz.,

TABLE VI. CI energies for low-lying vacancy states. Energies (in a.u.) are relative to the SCF energy of the  ${}^1E$  state. Changes in energy between different treatments are given in parentheses. A, self-consistent-field energies; B, CI including excitations among ( $a_1 t_2$ ) levels only; C, CI including B, plus excitations to virtual orbitals; D, total CI energy lowering; E, CI including C, plus excitations from deep valence levels.

	${}^1E$	${}^3T_1$	${}^1T_2$	${}^1A_1$	${}^5A_2$
A	0.0000 (0.076)	-0.0010 (0.067)	0.1016 (0.033)	0.1538 (0.037)	-0.0411
B	-0.0760 (0.006)	-0.0681 (0.006)	0.0688 (0.013)	0.1168 (0.013)	-0.0411 (0.004)
C	-0.0817 (0.006)	-0.0740 (0.010)	0.0557 (0.009)	0.1036 (0.008)	-0.0451 (0.005)
D	(0.088)	(0.083)	(0.055)	(0.058)	(0.009)
E	-0.0881	-0.0838	0.0464	0.0961	-0.0501

$${}^3T_1: \{[h_a(1)-h_b(1)][h_c(2)-h_d(2)]-[h_a(2)-h_b(2)][h_c(1)-h_d(1)]\} \frac{\alpha\beta+\beta\alpha}{\sqrt{2}}, \quad (28a)$$

$${}^1E: \{[h_a(1)-h_b(1)][h_c(2)-h_d(2)]+[h_a(2)-h_b(2)][h_c(1)-h_d(1)]\} \frac{\alpha\beta-\beta\alpha}{\sqrt{2}},$$

$${}^1T_2: \{[h_a(1)-h_b(1)][h_a(2)-h_b(2)]-[h_c(1)-h_d(1)][h_c(2)-h_d(2)]\} \frac{\alpha\beta-\beta\alpha}{\sqrt{2}}. \quad (28b)$$

Evidently the open-shell electrons in the  ${}^3T_1$  and  ${}^1E$  states occupy purely covalent distributions, while in the  ${}^1T_2$  state there are equal ionic and covalent contributions. Figure 9 illustrates the electronic distributions. The extensive ionic character of the  ${}^1T_2$  state raises questions about the adequacy of small cluster calculations to account for the proper splitting since the ionic distribution could lead to significant polarizations of the bulk orbitals and delocalization of the defect orbitals.<sup>10,28</sup>

In the SCF calculations there is some evidence of polarization of the bulk orbitals, but it is too small to have any significant effect on the energy splitting, nor does the CI lead to a reduced  ${}^1T_2$  and  ${}^3T_1$  splitting. It is possible that the atomic or-

bital basis might favor the ground state.<sup>11,29</sup> Although the  ${}^1T_2$  state is not highly excited, its ionic character could require a more spatially extended Rydberg-type description as is necessary for the Si  ${}^1S$  atomic state. Further local polarization effects and angular correlations could be important as well. Another possible concern is the cluster size itself which, it might be argued, is too small to support a proper  ${}^1T_2$  state.

To assess the questions of Rydberg-type contributions, or delocalization of the  ${}^1T_2$  state via dif-

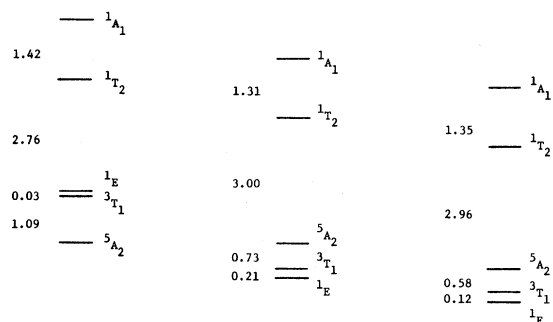


FIG. 8. Energy levels and splittings (in eV) of vacancy states for different treatments; (a) SCF, (b) CI including only defect level excitations, and (c) final CI.

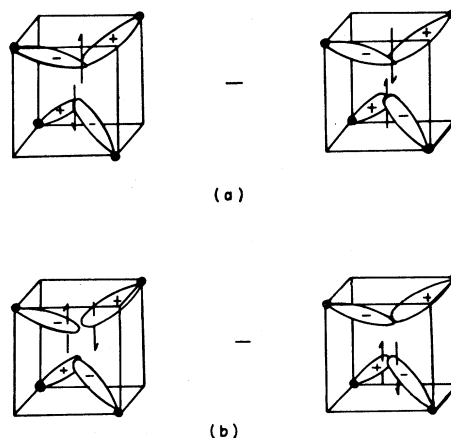


FIG. 9. Open-shell structure of the  ${}^3T_1$  and  ${}^1T_2$  vacancy states for  $s_z=0$ . The  ${}^1E$  state corresponds to a plus combination of the two  ${}^3T_1$  components.

fuse functions, a four-atom-Si model was investigated. The model consists of the four silicon atoms surrounding the vacancy in their unrelaxed geometry. The atoms are treated as effective one-electron atoms with the remaining electrons described in exactly the same manner as the boundary atom in the 16-atom cluster model. A triple-zeta basis is adopted by augmenting the previous ( $3s, 3s', 3p, 3p'$ ) basis with diffuse Gaussians ( $3s'', 3p''$ ) with exponent  $\alpha=0.05$ , orthogonalized to the core, and a single Gaussian (exponent  $\alpha=0.12$ ) of the  $d_{x^2-y^2}$  type with one lobe pointing along the bonding axis. The diffuse basis effectively extends outward by two neighbors, so that its utilization would correspond to extensive delocalization. The model thus permits the electronic distribution to utilize freely the spatially contracted, Rydberg and angular ( $d$ -orbital) components of the basis.

Initially, calculations with only the double-zeta basis are carried out to compare with the cluster results. The calculated  ${}^3T_1-{}^1T_2$  energy difference by SCF optimization is 0.121 a.u. compared to 0.101 a.u. for the large cluster. The discrepancy is due in part to the restricted  $s$ - $p$  ratio on the minimal basis components, and the forced localization over only four atoms.

Introducing the diffuse functions and  $d$  orbitals, the calculated  ${}^1T_2$  and  ${}^3T_1$  SCF energy difference is lowered to 0.089 a.u. The contribution of the diffuse and polarization basis is appreciable in the  $t_2$  orbitals optimized for the  ${}^1T_2$  state. Two different CI calculations were carried out with the orbital basis optimized for (a) the averaged configuration and (b) the  ${}^1T_2$  state. Table VII shows that

TABLE VII. CI energies of the  ${}^1T_2$  and  ${}^3T_1$  states of  $\text{Si}_4$ . Changes in energies between different treatments are given in parentheses. Energies are in a.u. Orbitals in the CI treatments are from averaged configuration and  ${}^1T_2$  optimized (see text). [ $\text{Si}_4\Delta({}^3T_1-{}^1T_2)=0.130$ ] A, self-consistent-field energies; B, CI including excitations among ( $a_1 t_2$ ) levels only; C, total CI energy lowering; D, CI including B, plus excitations to virtual orbitals.

	${}^1T_2^a$	${}^1T_2^b$	${}^3T_1^a$	${}^3T_1^b$
A	-2.3720 (0.026)	-2.3815 (0.020)	-2.4639 (0.062)	-2.4516 (0.044)
B	-2.3980 (0.027)	-2.4018 (0.024)	-2.5258 (0.027)	-2.4957 (0.052)
C	(0.053)	(0.044)	(0.089)	(0.096)
D	-2.4249	-2.4253	-2.5530	-2.5475

<sup>a</sup> $\Delta({}^3T_1-{}^1T_2)=0.128$ , averaged configuration.

<sup>b</sup> $\Delta({}^3T_1-{}^1T_2)=0.122$ ,  ${}^1T_2$  state orbitals.

both calculations produce essentially the same final configuration interaction energy. Although these results are similar to those of the cluster for the CI lowering due to excitations among defect orbitals, the lowerings due to excitations to the virtual space are different due to the extensive basis used in the present treatment.

Nonetheless, after the final CI treatment the splittings in both treatments are in essential agreement with those obtained for the cluster. This suggests that the omission of diffuse functions from the basis is not a serious limitation on the accuracy of the calculated states of the large cluster.

## VI. DISCUSSION AND CONCLUSIONS

### A. Comparison to other theoretical work

Cluster calculations on the silicon vacancy similar to the present work have been performed by Surratt and Goddard.<sup>9,28</sup> Aside from technical differences in the methods, there are essential differences in the models used. The Surratt and Goddard method of cluster termination employs hydrogen atoms at the Si-H bond distance appropriate to the  $\text{SiH}_4$  molecule, and the four silicon atoms have been slightly relaxed from the equilibrium lattice position. They predict the three lowest-lying states to be ordered as  ${}^1E < {}^3T_1 < {}^5A_2$  with energy separations of 0.18 and 0.60 eV above the  ${}^1E$  state. These results are in good agreement with the present results (Fig. 8) and we concur with their conclusion that electron correlation is essential in determining the correct ground state. Our  ${}^1T_2$  state is  $\sim 0.40$  eV lower than their uncorrected value.<sup>28</sup> Because of the large dipole moment they calculate for this state, a classical model is used to estimate the lowering due to polarization of the infinite solid. We have, however, found no evidence in  $\text{Si}_{17}$  of such substantial polarizations.

The present SCF results are in qualitative agreement with the findings of Baraff and Schlüter using Green's-function methods.<sup>5</sup> They report two resonance levels (defect-related orbitals embedded within the occupied band) of  $a_1$  symmetry. The lower level is primarily  $s$  type while the higher is primarily  $p$  type, which matches the characteristics of our  $1a_1$  and  $2a_1$  orbitals. Their energy difference between these two levels is 7.3 eV as opposed to the present value of 11.2 eV. They also report a  $t_2$ -symmetry bound level (i.e., embedded in the gap) at 1.7 eV above the higher resonance level. In all our SCF calculations the highest occupied levels

were of the  $t_2$  type; in particular, the  $3t_2$  levels optimized for the  ${}^3T_1$  gave the same eigenvalue difference. It is noted, however, that in their calculation the occupancy of the bound  $t_2$  level is treated in the same fashion as the averaged configuration here.

Lannoo *et al.* have calculated multiplet splittings for the unrelaxed silicon vacancy<sup>7</sup> using a perturbation expansion within the local-density formalism.<sup>30</sup> The splitting scheme they obtain corresponds to that of our SCF results (see Sec. V B) except in the value for the exchange interaction. Their spectrum depends on two energy parameters  $E'_{\rho_0}$  and  $E'_v$  which can be related to conventional Hartree-Fock integrals as<sup>30</sup>

$$(t_x t_y || t_x t_y) = E'_{\rho_0} - 2E'_v, \quad (29a)$$

$$(t_x t_x || t_x t_x) - (t_x t_x || t_y t_y) = 6E'_v, \quad (29b)$$

so that using our values we find (in a.u.)

$$E'_v = 0.00017, \quad (30a)$$

$$E'_{\rho_0} = 0.0516, \quad (30b)$$

while their estimated values are

$$E'_v = 0.00012, \quad (31a)$$

$$E'_{\rho_0} = 0.01210. \quad (31b)$$

Thus, we are at variance in the calculation of the parameter  $E'_{\rho_0}$ , which differs by a factor of 4.26. The evaluation of Lannoo *et al.* of this integral involves the product of the averaged bound  $t_2$  level density and the density derivative of a Slater  $X\alpha$ -type local exchange potential. It is therefore not clear whether the discrepancy between calculated values is due to the description of the bound  $t_2$  orbitals or the potential used to evaluate the integral. Since they include no correlation via many electron excitations to correct the Hartree-Fock splittings, they obtain a different ordering of the  ${}^1E$  and  ${}^3T_1$  levels. At the SCF level neither of these is the ground state, but it is the  ${}^5A_2$  state which is not considered in their formalism.

The open-shell contributions to both the  ${}^1E$  and  ${}^3T_1$  states correspond to covalent configurations when viewed in terms of the proper symmetry combination of determinants (see Fig. 9). However, the doubly occupied  $a_1$  orbital contributes both ionic and covalent distributions in a fixed ratio at the minimal configuration (SCF) level. The primary purpose of configuration interaction is to achieve the proper ionic-covalent balance and both the  ${}^1E$  and  ${}^3T_1$  states are found to interact strongly

with excitations among the defect orbitals. The  ${}^1T_2$  state, although ionic with respect to the  $t^2$  configuration, is not as significantly altered by defect orbital excitations (the leading determinant retains a large coefficient,  $\sim 0.94$ ). Thus CI greatly affects the relative ordering of the low-lying defect states.

Experimentally much information about the silicon vacancy has been acquired by electron spin resonance (ESR) studies, although, since the neutral vacancy has no net spin, its structure is inferred indirectly either from known structure about the charged vacancy states<sup>31</sup> or by its interaction with an impurity.<sup>32</sup> The evidence is interpreted to suggest that the lowering in energy due to Jahn-Teller distortions is more important than many-body effects.<sup>33</sup> Since we have, at present, only treated the unrelaxed vacancy, our only contention in this regard is that electronic correlation is important for the nuclei in their unrelaxed positions. For small relaxations the correlation contributions are not expected to diminish appreciably.<sup>34</sup> However, more quantitative information requires actual computations on the relaxed vacancy. These studies are underway.

## B. Conclusion

We have examined in detail the electronic structure of the unrelaxed neutral silicon vacancy. We confirm the basic results of Surratt and Goddard<sup>9</sup> insofar as the description of low-lying  ${}^1E$ ,  ${}^3T_1$ , and  ${}^5A_2$  states; we have, however, found no evidence in our calculations that the  ${}^3T_1$ - ${}^1T_2$  splitting is reduced by polarization effects. We have carefully assessed the effects that lower these two states and have found that the favored lowering of the  ${}^3T_1$  versus the  ${}^1T_2$  is not due to a deficiency in the basis, but is a real effect due to the covalent nature of the  ${}^3T_1$  state as opposed to the covalent plus ionic nature of the  ${}^1T_2$  state. For nuclei in their unrelaxed positions, correlation effects are found to be absolutely essential in sorting out the relative ordering between the  ${}^1E$  and  ${}^3T_1$  states.

## ACKNOWLEDGMENTS

We are grateful for the services provided by the State University of New York (SUNY) Computing Center at Stony Brook in facilitating this study. Partial support of this research by the U.S. Department of Energy (Contract No. DEAC0277-ER04387) is gratefully acknowledged.

- <sup>1</sup>G. F. Koster and J. C. Slater, *Phys. Rev.* **95**, 1167 (1954).
- <sup>2</sup>J. Callaway, *J. Math. Phys.* **5**, 783 (1964).
- <sup>3</sup>J. Bernholc, N. O. Lipari, and S. T. Pantelides, *Phys. Rev. B* **21**, 3545 (1980).
- <sup>4</sup>M. Jaros, C. O. Rodriguez, and S. Brand, *Phys. Rev. B* **19**, 3137 (1979).
- <sup>5</sup>G. A. Baraff and M. Schlüter, *Phys. Rev. B* **19**, 4965 (1979).
- <sup>6</sup>G. A. Baraff, E. O. Kane, and M. Schlüter, *Phys. Rev. B* **21**, 5662 (1980).
- <sup>7</sup>M. Lannoo, G. A. Baraff, and M. Schlüter, *Phys. Rev. B* **24**, 955 (1981).
- <sup>8</sup>C. A. Coulson and M. J. Kearsley, *Proc. R. Soc. London Ser. A* **241**, 433 (1957).
- <sup>9</sup>G. T. Surratt and W. A. Goddard III, *Phys. Rev. B* **18**, 2831 (1978).
- <sup>10</sup>M. Lannoo, in *International Conference on Radiation Effects in Semiconductors, Nice, 1978*, edited by J. H. Albany (IOP, London, 1979), p. 1.
- <sup>11</sup>J. L. Whitten and T. A. Pakkanen, *Phys. Rev. B* **21**, 4357 (1980).
- <sup>12</sup>B. Cartling, B. Roos, and U. Wahlgreen, *Chem. Phys. Lett.* **21**, 380 (1979).
- <sup>13</sup>J. L. Whitten, *Acc. Chem. Res.* **6**, 238 (1973), and references therein.
- <sup>14</sup>C. C. J. Roothaan, *Rev. Mod. Phys.* **23**, 69 (1951).
- <sup>15</sup>J. C. Phillips and L. Kleinman, *Phys. Rev.* **116**, 287 (1959).
- <sup>16</sup>J. L. Whitten and M. Hackmeyer, *J. Chem. Phys.* **51**, 5584 (1969).
- <sup>17</sup>T. H. Dunning, Jr. and P. J. Hay, in *Methods of Electronic Structure Theory*, edited by H. F. Schaeffer III (Plenum, New York, 1977).
- <sup>18</sup>J. L. Whitten, *J. Chem. Phys.* **39**, 349 (1963) and H. Le Rouzo and B. Silvi, *Int. J. Quantum Chem.* **13**, 297 (1978).
- <sup>19</sup>B. Roos and P. Siegbahn, *Theor. Chim. Acta* **17**, 209 (1970).
- <sup>20</sup>A. Veillard, *Theor. Chim. Acta* **12**, 405 (1968).
- <sup>21</sup>M. Weissbluth, *Atoms and Molecules* (Academic, New York, 1978), pp. 242-243.
- <sup>22</sup>C. E. Moore, *Atomic Energy Levels*, Natl. Bur. Stand. (U.S.) Spec. Publ. No. 323 (U.S. G.P.O., Washington, D.C., 1949).
- <sup>23</sup>E. O. Kane and A. B. Kane, *Phys. Rev. B* **17**, 2631 (1978).
- <sup>24</sup>J. C. Phillips, *Bonds and Bands in Semiconductors*, (Academic, New York, 1973), p. 115.
- <sup>25</sup>J. R. Chelikowsky and M. L. Cohen, *Phys. Rev. B* **14**, 556 (1976).
- <sup>26</sup>J. R. Chelikowsky and M. L. Cohen, *Phys. Rev. B* **10**, 5095 (1974).
- <sup>27</sup>A. C. Kenton and M. W. Ribarsky, *Phys. Rev. B* **23**, 2897 (1981).
- <sup>28</sup>G. T. Surratt and W. A. Goddard III, *Solid State Commun.* **22**, 413 (1977).
- <sup>29</sup>J. L. Whitten, *J. Chem. Phys.* **56**, 5458 (1972).
- <sup>30</sup>M. Lannoo, G. A. Baraff, and M. Schlüter, *Phys. Rev. B* **24**, 543 (1981).
- <sup>31</sup>G. D. Watkins, J. R. Troxell, and A. P. Chatterjee, in *International Conference on Radiation Effects in Semiconductors, Nice, 1978*, edited by J. H. Albany (IOP, London, 1979), p. 16.
- <sup>32</sup>G. D. Watkins and J. W. Corbett, *Phys. Rev.* **134A**, 1359 (1964).
- <sup>33</sup>G. D. Watkins, *J. Phys. Soc. Jpn. Suppl.* **2**, 22 (1963).
- <sup>34</sup>H.-O. Beckmann, J. Koutecký, and V. Bonačič-Koutecký, *J. Chem. Phys.* **73**, 5182 (1980).